JOURNAL OF PROPULSION AND POWER
Vol. 21, No. 5, September–October 2005

New Kinetics for a Model of Heterogeneous Propellant Combustion

L. Massa,* T. L. Jackson,† and J. Buckmaster‡
University of Illinois at Urbana–Champaign, Urbana, Illinois 61801

In earlier work we describe an unsteady, three-dimensional, phase-coupled combustion code which, with the use of a random packing algorithm to construct model propellants, and the use of a homogenization strategy to account for unresolvably small propellant particles, can be used for the simulation of heterogeneous propellant combustion. This work uses a simple two-step kinetic model for ammonium perchlorate (AP)/hydroxyl-terminated polybutadiene (HTPB) combustion which fails to accurately predict variations in the burning rate with AP concentration for a homogenized AP/HTPB blend supporting a one-dimensional flame. Here we describe a three-step model, one which captures the three flames of the Beckstead-Derr-Price (BDP) combustion model, and show that kinetic parameters can be adopted so that one-dimensional AP burning rates and one-dimensional AP/HTBP blend burning rates can be correctly predicted. We discuss the stability of the underlying flame structures and highlight a difficulty that arises in these instability-prone systems when simple kinetic models are used to describe them. The combustion model, with the new kinetics, is used to reexamine the burning of random packs, and improved agreement with the experimental burning rates of Miller packs is demonstrated. We also reexamine the problem of sandwich-propellant combustion and investigate the trend in surface shape and burning-rate variations with pressure and binder width. These trends are compared with experimental results of Price. The sandwich configuration is used to measure the importance of the primary diffusion flame of the BDP model.

Nomenclature

$A_{\mathrm{AP},B,\mathrm{blend}}$	=	pyrolysis rate constants
c_p	=	specific heat
$D_{1,2,3}$	=	reaction rate constants
$E_{\mathrm{AP},B,\mathrm{blend}}$	=	pyrolysis activation energies
$E_{1,2,3}$	=	gas phase reaction activation energies
f	=	surface function
M	=	mass flux
MW	=	molecular weight
$\boldsymbol{n}$	=	surface normal
$n_{1,2,3}$	=	pressure exponents in the reaction rates
P_0	=	spatially invarient background pressure
Pr	=	Prandtl number
p	=	spatially varying flow pressure
$Q_{g1,g2,g3}$	=	heats of reaction
Q_s	=	heat of decomposition
$R_{1,2,3}$	=	gas phase reaction rates
R_u	=	universal gas constant
r_b	=	surface regression rate
T	=	temperature
T_0	=	supply temperature of the solid
t	=	time
u, v, w	=	velocity components
X	=	mass fraction of AP in the gas phase
x, y, z	=	Cartesian coordinates
Y	=	mass fraction of binder gases
Z	=	mass fraction of AP decomposition products
β	=	mass-based stoichiometric coefficient
η	=	mapping function
λ	=	heat conductivity
ρ	=	density
$()_{\mathrm{AP}}$	=	ammonium perchlorate
$()_B$	=	binder
$()_{\mathrm{blend}}$	=	AP/binder blend
$()_c$	=	condensed phase
$()_g$	=	gas phase
$()_s$	=	surface

Received 14 May 2003; accepted for publication 21 April 2004.

*Postdoctoral Associate, Center for Simulation of Advanced Rockets, 1304 West Springfield Avenue.

†Senior Research Scientist, Center for Simulation of Advanced Rockets, 1304 West Springfield Avenue. Member AIAA.

‡Professor, Department of Aerospace Engineering, 104 South Wright Street; limey@uiuc.edu. Associate Fellow AIAA.

I. Introduction

WE are concerned with the numerical calculation of the combustion field supported by heterogeneous propellants that consist of ammonium perchlorate (AP) particles embedded in a fuel binder, specifically hydroxyl-terminated polybutadiene (HTPB). Such propellants are widely used in the rocket industry, for example in the Space-Shuttle boosters, and more scientific strategies than those used hitherto to predict their performance could serve vital national needs. Applications of our work include the development of equivalent one-dimensional formulations for use in whole-rocket simulations,[1] and the examination of the burning response to acoustically generated pressure disturbances.[2]

In recent years we have developed a number of tools that, for the first time, enable us to address this problem in a reasonably sophisticated fashion, incorporating three-dimensional effects, a random pack model of the propellant,[3,4] and complete coupling of the gas-phase combustion processes and the solid-phase heat conduction across the unsteadily regressing nonplanar propellant surface. Numerical limitations inherent in a problem of this complexity do not permit us to resolve the smallest AP particles, often present in significant volume, and we have developed a rational homogenization strategy to account for the role that these particles play in defining the thermal conductivity of the solid and the pyrolysis law that characterizes the surface regression rate.[5] Application of these tools to the burning of random pack propellants can be found in Refs. 6 and 7, and to the burning of sandwich propellants in Ref. 8. We note here that our main focus has been, and still is, on tool development, rather than the massaging of parameter values to fit the limited experimental data, an issue that we discuss later in this paper, but to a significant extent

our parameter choices have their roots in experiment. This has enabled us, for example, to meaningfully compare the burning rates of model Miller packs[9] with experimental burning rates.[7] The code, as first implemented, can not accommodate steep or multivalued surface profiles, but recently we have developed a level-set strategy that overcomes this limitation, work that is reported in Ref. 10. In the present paper the surface slope is always modest, so that the original strategy, in which the surface is mapped onto a plane, suffices.

The chemical kinetics adopted in Refs. 6–8 is two-step in nature, allowing for AP decomposition and the combustion of the decomposition products with binder gases. The so-called primary diffusion flame of the Beckstead-Derr-Price model,[11] one supported by virgin AP gases and binder gases, is not accomodated. The two-step model has significant advantages in that the limited number of parameters needed for its specification can be chosen to fit one-dimensional burning rates (of pure AP and of a homogenized blend of 80% AP and binder) and their sensitivities (to supply temperature) with no redundancy. At all times we have avoided using data from multidimensional burning experiments to determine parameter choices, as we wish to reserve such data for model validation.

A disadvantage of the two-step kinetics model is that, although we can fit the one-dimensional burning rate for a single blend, we cannot correctly match variations of this burning rate with variations in the AP fraction. This has been of some concern to us as the random pack calculations[7] make significant use of homogenization, and the homogenized matrix in which the larger AP particles are embedded varies widely in composition. For this reason we have been motivated to add a "primary diffusion flame" component to the two-step model to create a three-step model, and we have chosen the parameters of this model to match pure AP burning and blend burning over a range of compositions.

The structure of the paper is as follows. We describe the ingredients of the fully-coupled problem of propellant burning, with details of the three-step kinetic scheme and its validation via 1-dimensional calculations. Stability issues are discussed, and provide a cautionary note whenever simple ad hoc kinetic schemes are adopted for instability-prone systems in combustion. We examine the burning of random-pack propellants and recalculate burning-rate-pressure variations for a number of Miller packs,[9] with better agreement than that afforded by two-step kinetics. Finally we examine the burning of sandwich propellants, and discuss how the surface shape and the burning-rate vary with pressure and binder thickness, variations that are compared with experimental results of Price et al.[12] Sandwich calculations are also used as a platform to examine the importance of the primary diffusion flame.

II. Fully-Coupled Problem of Propellant Burning

A full description of the numerical model can be found in our earlier work,[6,7] but here we sketch its essential details. The computational strategies are described in Ref. 13.

Condensed Phase

In the condensed phase we solve the heat equation

$$c_p \rho_c \frac{\partial T}{\partial t} = \nabla \cdot (\lambda_c \nabla T) \tag{1}$$

where we assume, for simplicity, that the specific heat is the same as that for the gas; the values of ρ_c and λ_c (pointwise constants) are assigned according to whether a point is located in the binder or in an AP particle. When the binder is replaced by a homogenized AP/binder blend, λ is defined by the homogenization formulas that can be found in Ref. 5, different formulas according to whether the problem is two-dimensional or three-dimensional.

Propagation of the Surface

The surface regresses normal to itself with a speed r_b (>0), where we assume that r_b is defined by simple pyrolysis laws, viz.

$$r_b = \begin{cases} r_{\mathrm{AP}} = A_{\mathrm{AP}} \exp\{-E_{\mathrm{AP}}/R_u T_{\mathrm{AP},s}\} & \text{in the AP} \\ r_B = A_B \exp\{-E_B/R_u T_{B,s}\} & \text{in the binder} \end{cases} \tag{2}$$

where $T_{,s}$ is the surface temperature. Also, if the binder is replaced by a blend the homogenization formulas from Ref. 5 must be used for parameters A_{blend}, E_{blend}.

It is convenient to represent the surface by

$$y = f(x, z, t) \tag{3}$$

where f, the surface location, is a single-valued function of (x, z). Thus, y is nominally measured perpendicular to the propellant surface, and x and z are nominally measured parallel to the surface. (Should f not be single valued-should a portion of the surface overhang another portion-an alternative strategy is required, which is described in Ref. 10.) Surface kinematics leads to the following equation:

$$f_t + r_b \sqrt{1 + f_x^2 + f_z^2} = 0 \tag{4}$$

Gas-Phase

Gas-phase processes are described by the zero-Mach-number Navier–Stokes equations for a variable-density gas, the energy equation, species equations, and suitable chemical kinetics. An Oseen approximation, which enables us to discard the momentum equation, has proven remarkably accurate[6,7] and often suffices for our purposes, but the results that we report here do not use it.

We use a simple three-step kinetics scheme, represented by

$$\begin{aligned} \mathrm{AP}(X) &\xrightarrow{R_1} \text{decomposition products}(Z) \\ \beta X + \text{binder}(Y) &\xrightarrow{R_2} \text{final products} \\ \beta Z + \text{binder}(Y) &\xrightarrow{R_3} \text{final products} \end{aligned} \tag{5}$$

where

$$\begin{aligned} R_1 &= D_1 P_0^{n_1} X \exp(-E_1/R_u T) \\ R_2 &= D_2 P_0^{n_2} X^{3.3} Y^{0.4} \exp(-E_2/R_u T) \\ R_3 &= D_3 P_0^{n_3} Y Z \exp(-E_3/R_u T) \end{aligned} \tag{6}$$

We assume that the products of the reactions R_2 and R_3 are identical, so that the system has a well-defined path-independent equilibrium state [see Eq. (17)].

Note that, with two global reactants, one of which can support a decomposition flame, the global system (5) is a natural choice and is used in the well known BDP model.[11] In our earlier work, R_2, corresponding to the primary diffusion flame, was neglected, and one of the things that we discuss in this paper is its importance. It should also be noted that Beckstead has long believed that the primary diffusion flame is important, a belief implied in Ref. 14, and clearly expressed in Refs. 15 and 16.

The corresponding equations for X, Y, Z and T are

$$\mathcal{L}(X, Y, Z) = (-R_1 - \beta R_2, -R_2 - R_3, R_1 - \beta R_3) \tag{7}$$

$$\mathcal{L}(T) = \frac{(Q_{g1} R_1 + Q_{g2} R_2 + Q_{g3} R_3 + d P_0/dt)}{c_p} \tag{8}$$

where

$$\mathcal{L} \equiv \rho \frac{D}{Dt} - \nabla \cdot [(\lambda_g/c_p) \nabla] \tag{9}$$

We have assumed that all Lewis numbers are equal to 1, but temperature dependent transport is accounted for[17]

$$\lambda_g = 1.08 \times 10^{-4} T + 0.0133 \text{ W/m K} \tag{10}$$

when T is assigned in degrees Kelvin; c_p is assumed to be constant.

The parameter β in Eqs. (5) and (7) is the overall mass-based AP/binder stoichiometric ratio: β kg of AP(X) are required for the stoichiometric consumption of 1 kg of binder (Y). Later we shall describe how the kinetics parameters of Eqs. (6) are determined.

The remaining equations are

$$P_0(t) = \frac{\rho R_u T}{MW} \tag{11}$$

$$\frac{\partial \rho}{\partial t} + \nabla \cdot (\rho \boldsymbol{q}) = 0, \qquad \boldsymbol{q} = (u, v, w) = (q_1, q_2, q_3) \tag{12}$$

$$\rho \frac{Dq_i}{Dt} = -\frac{\partial p}{\partial x_i} + \frac{\partial}{\partial x_j}\left(\frac{Pr\lambda_g}{c_p}\frac{\partial q_i}{\partial x_j}\right) + \frac{\partial}{\partial x_j}\left(\frac{Pr\lambda_g}{c_p}\frac{\partial q_j}{\partial x_i}\right) - \frac{2}{3}\frac{\partial}{\partial x_i}\left(\frac{Pr\lambda_g}{c_p}\frac{\partial q_k}{\partial x_k}\right) \tag{13}$$

where the Prandtl number is assumed to be constant.

Conditions at the Propellant Surface

The propellant surface is an interface between the condensed phase and the gas phase, and certain conditions are imposed there which relate the solution in one phase to that in the other. These include continuity of tangential velocity (zero in the solid, and therefore zero in the gas) and continuity of normal mass flux ($\rho_c r_b$ in the solid).[6] Energy conservation at the surface has the form

$$[\lambda \boldsymbol{n} \cdot \nabla T] = -Q_s M \tag{14}$$

and the species flux condition is

$$M[Y_i] = [(\lambda/c_p)\boldsymbol{n} \cdot \nabla Y_i] \tag{15}$$

In all of these formulas $[\,] \equiv (\,)_g - (\,)_c$; Y_i refers to the species X, Y or Z; M is the mass flux normal to the surface; $Q_s > 0 (< 0)$ for an exothermic (endothermic) process; and both r_b and Q_s take on different values according to whether the surface is AP, binder, or blend. It is computationally convenient to deal with the unevenness of the surface by use of the mapping

$$x, y, z, t \to x, \eta = y - f(x, z, t), z, t \tag{16}$$

so that the surface is flat in the new coordinates. This is used to transform both the field equations and the surface conditions.

Defining Kinetics Parameters

Table 1 shows the parameter choices that we have made, and many of them are identical to those used in Refs. 6 and 7, but the kinetics scheme is here quite different and the parameters are fixed in the following fashion.

The key information that we use comes from the burning of pure AP and the burning of a homogenized blend of AP and binder. In both cases the flames are deflagrations; there are extensive experimental data for the first (e.g., Ref. 18), and complex-kinetics numerical data for the second, supplemented by a small amount of experimental data.[19]

The AP decomposition is defined purely by R_1, and the parameters of that reaction are chosen to match steady burning rates and the sensitivity of the burning rate to supply temperature variations. In the earlier work, sensitivity was estimated using formulas deduced from large-activation-energy asymptotics, but it so happens that the error in doing this is substantial, and here we calculate the sensitivity numerically. Values vary between 2.6×10^{-3} and 2.8×10^{-3} in the pressure interval 20–80 atm, in good agreement with established values.

Table 1 Parameter values

Head	Head
A_{AP}	1.45×10^5 cm/s
A_B	1.036×10^3 cm/s
c_p	0.3 kcal/kg K
D_1	4.11×10^1 gm/cm^3 s bar^{n_1}
D_2	2.35×10^4 gm/cm^3 s bar^{n_2}
D_3	9.5×10^1 gm/cm^3 s bar^{n_3}
E_{AP}/R_u	11000 K
E_B/R_u	7500 K
E_1/R_u	3000 K
E_2/R_u	8500 K
E_3/R_u	8500 K
MW	26
n_1	2.06
n_2	2.06
n_3	1.60
Pr	1
Q_{g1}	410 kcal/kg
Q_{g2}	7403 kcal/kg
Q_{g3}	4396 kcal/kg
$Q_{s,\mathrm{AP}}$	−80 kcal/kg
$Q_{s,B}$	−66 kcal/kg
R_u	1.9859 kcal/kmol K
T_0	300 K
β	7.33
λ_{AP}	0.405 W/m K
λ_B	0.276 W/m K
ρ_{AP}	1950 kg/m^3
ρ_B	920 kg/m^3

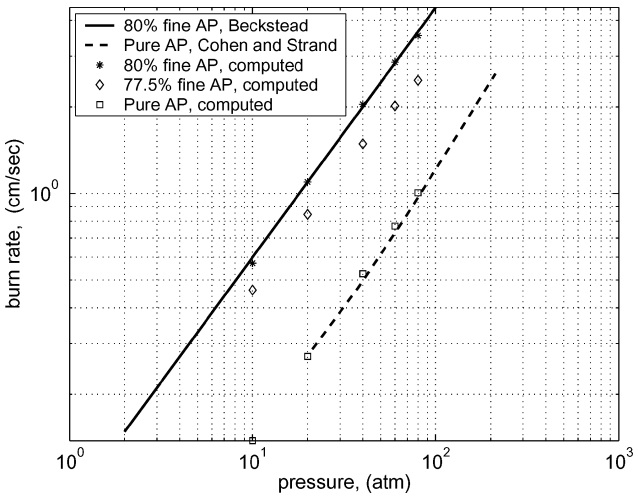

Fig. 1 Burning rate vs pressure for pure AP and various AP/binder blends.

The activation energy is markedly lower than the one used in our earlier studies because of the different way in which the sensitivity is calculated. The implications of this for some of our earlier results will be discussed elsewhere, but it is worth noting that we use the sensitivity to fix AP kinetics parameters, not because that generates an optimal model but because it is one of the few global parameters that is known. Matching the burning rate and its first derivative (with respect to supply temperature) enables us to determine D_1 and E_1, but it does not follow that those are the best choices for capturing, say, the dynamic response of the burning rate to transient disturbances. The question: 'What are the best parameter choices for simple kinetic models?,' is not well posed. This point will be emphasized again later, when we discuss the one-dimensional stability of AP/binder blends.

Predicted AP burning rates vs pressure are compared with the experimental values of Ref. 18 in Fig. 1. This figure also shows steady burning rates for various AP/binder blends, which we discuss next.

The parameters for the R_2 and R_3 reactions are chosen to match the burning rates of AP/binder blends predicted by Jeppson et al.[19]

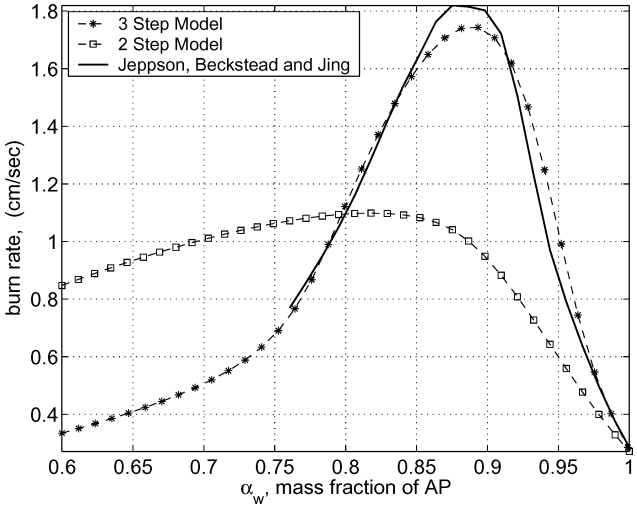

Fig. 2 Burning rate vs AP fraction for an AP/binder blend; pressure = 20 atm.

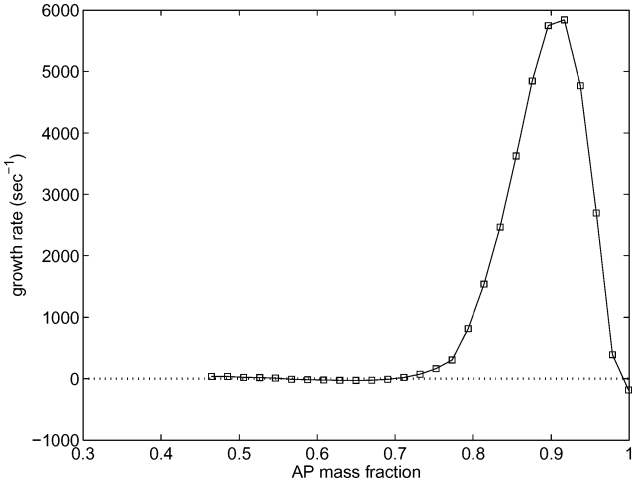

Fig. 3 Growth rate of linear disturbances for a 1-dimensional flame supported by an AP/binder blend; pressure = 20 atm.

Note the dependence of R_2 on X and Y. The process that leads to these values is guided by parameter-sensitivity calculations, but there is also a random component and all that can be reasonably said is that the comparisons are good (Fig. 2), yet the choices are not unique. No sensitivity data are used in making these choices.

Note from Fig. 2 that the three-step model reasonably captures variations of the burning rate with AP concentration, whereas the two-step model does not. The latter deficiency has been of some concern to us since in carrying out three-dimensional random-pack burning calculations it is necessary to homogenize the smaller AP particles into the binder, and the correct capture of the burning rate of such blends could be important.

Other Parameters

The stoichiometric parameter β is assigned the value 7.33 (Ref. 19) corresponding to an AP mass fraction of 0.88 in a stoichiometric configuration. The adiabatic flame temperature for pure AP is 1400 K, that for a stoichiometric AP/binder blend is 3000 K,[19] and the Q_{gi} are chosen accordingly. Note that

$$Q_{g3} = Q_{g2} - \beta Q_{g1} \tag{17}$$

to ensure that the equilibrium temperature is a state variable and is not path dependent. As in Ref. 20 the AP pyrolysis parameters are chosen so that the surface temperature at the low-pressure AP deflagration limit is equal to a melting temperature of 834 K.

III. One-Dimensional Stability of Deflagrations Supported by Blends

It has long been known that deflagrations supported by propellants can exhibit oscillating instabilities, an issue extensively discussed in Ref. 21; a useful discussion can also be found in Ref. 22. For a one-dimensional combustion field in which the gas-phase is quasi-steady, the linear stability characteristics can be deduced by using a numerical strategy in the gas phase, and an analytical strategy in the solid phase.

The solution in the gas phase is controlled exclusively by the surface temperature T_s: with T_s assigned, the mass flux is fixed by the pyrolysis law, and the surface reactant fluxes are fixed by surface conservation laws. Thus, the steady equations can be integrated to determine the heat flux to the surface, and in this way the temperature gradient on the solid side of the surface can be calculated. If we denote this by $g(T_s)$, then a straightforward linear stability analysis within the solid, with disturbances $\sim e^{at}$, yields the following formula for a:

$$a\tau_c = -\theta + \tfrac{1}{2}(G' - 1)\left[G' \pm \sqrt{G'^2 - 4\theta}\,\right] \tag{18}$$

where

$$\theta = \frac{E_{\text{blend}}(T_s - T_0)}{RT_s^2}, \qquad G' = L_c \frac{dg}{dT_s} \tag{19}$$

and L_c is the characteristic length $\lambda_c/\rho_c r_b c_p$ and τ_c is the characteristic time L_c/r_b. G' is determined by numerical differentiation of g.

In Fig. 3, the real part of a (the growth rate) is plotted as a function of the AP mass fraction of the blend for a pressure of 20 atm, and this shows a strong instability for mass fractions greater than about 0.7, not including a small neighborhood of 1 (pure AP). We show no two-step results of this kind here, but they are quite different; apparently the R_2 reaction plays an important role in the determination of the heat flux to the surface (and thus G').

We do not know if the instability revealed by Fig. 3 is real or not, but we can be sure that the numbers are wrong. The only way they could be right is if the kinetics model were chosen to match not only known burning rates, but known sensitivities, here the sensitivity of the surface heat flux to surface temperature, for different AP fractions. Whether this matters or not depends on what the model is used for, but we note that instability of a steadily burning propellant can lead to a mean burning rate that differs significantly from the steady value.

IV. Burning of Random-Pack Propellants

We define a propellant pack by a periodic array of cubes, each randomly packed as in the pack shown in Fig. 4. To describe the burn-through of a single cube, one or more cubes are first consumed to ensure that periodic burning has been achieved, that the consumption of the cube is independent of the initial conditions.

Earlier[7] we reported on the burning of packs constructed to represent Miller packs, real packs constructed and burnt by R. Miller,[9] and in Fig. 5 we show those earlier results together with the predictions of the three-step model. The details of the packs may be found in Ref. 7 but we note here the volume fraction of AP in the homogenized matrix in which pure AP particles are embedded: M03, 0.569; M17, 0.323; M21, 0.425; M24, 0.257.

The three-step model gives noticeably better agreement with experiment than the two-step model for M03; for M17 the excellent agreement between the two-step model and experiment is unchanged; the three-step model gives improved agreement at the lower pressures for M21, but we note, by a comparison with pure AP burning shown on the same panel, that the experimental results appear to be anomalous; and for M24 the three-step model gives improvement. Note that the numerical results for M21 appear to asymptote the pure AP burning curve at the higher pressures, as expected. Note also that for M03 the mass fraction of AP in the matrix blend is 0.74, which puts it in the unstable domain defined by Fig. 3, and it is perhaps for this reason that the numerical data do not lie on a simple curve.

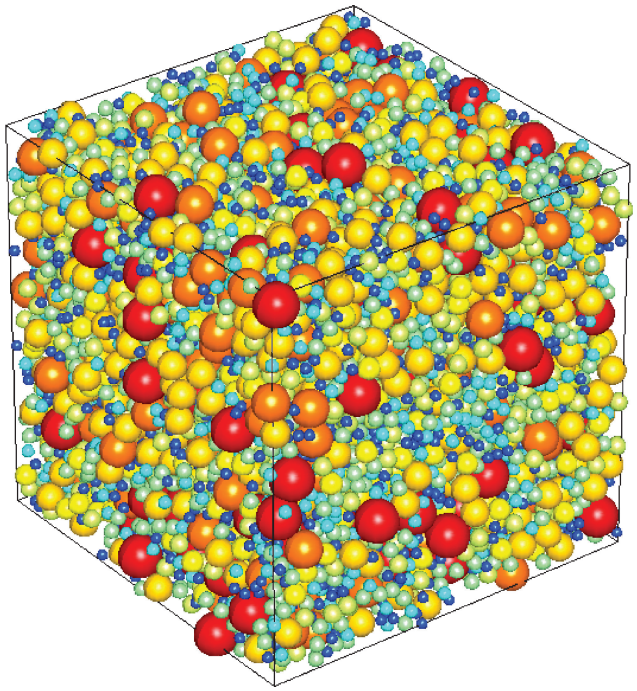

Fig. 4 A 10,001 particle pack that models the Miller M21 pack,[9] courtesy of S. Kochevets. For the numerical simulations, packs containing 3002 particles are used in a cube of side 1731.79 μm.

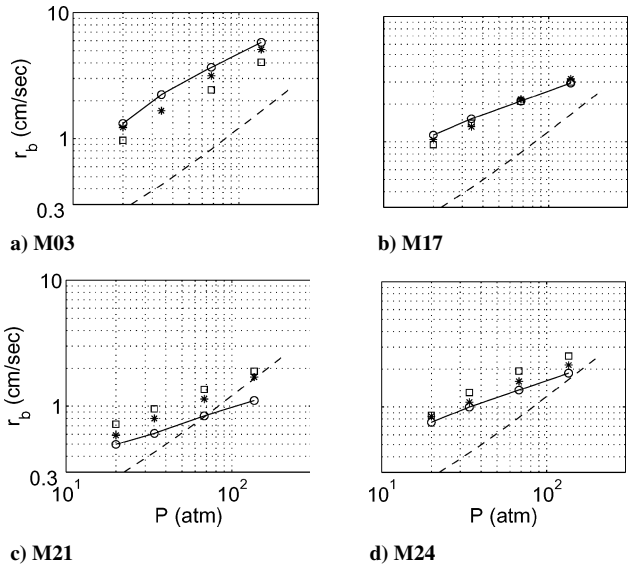

Fig. 5 Mean burning rate vs. pressure for four Miller packs M03, M17, M21, and M24[9]: ○, experimental; □, numerical, 2-step kinetics; ∗, numerical, 3-step kinetics. Pure AP burning is shown by broken lines.

The errors correlate with the AP size in the following sense: For M03, for which the larger AP particles are roughly 20 μm in diameter, the numerics underpredicts the burning rate; for M17, 90 μm, the error is negligible; and for M24, 200 μm, there is overprediction. This trend continues with M21, for which the larger particles are roughly 450 μm in diameter.

These results are encouraging, particularly in view of the fact that none of the parameters have been chosen to fit multidimensional experimental data. If we discount the M21 results, we can reasonably claim that the model provides a decent estimate of the effects of propellant morphology on steady burning rates in the pressure range 20 to 136 atmospheres. These effects are not small: M03 burns up to 3 times faster than M24, Fig. 5. We now turn to some of the details of the combustion field and the burning process.

Figure 6 shows the evolution of the M21 propellant surface at four different pressures. The time interval between consecutive traces is approximately 10^{-3} s, and so the spacing increases with increasing pressure and increasing burning rate. The large AP particles always protrude above the surrounding surface, particularly in their final moments, but this is less noticeable at the higher pressures, so that at 136 atm, for example, the surface remains fairly flat. It is apparent from Fig. 5 that the difference between the burning rate of the pack and that of pure AP diminishes with increasing pressure. This is consistent with the idea, suggested by the 20 atm profiles of Fig. 6, that the surface near the center of the large AP particles is struggling to keep up with the overall regression, and surface curvature plays a key role in making this possible, focusing the heat flux in the thermal-diffusion layer in the solid. This focusing effect is one we shall also see in the sandwich propellant results.

Figure 6 corresponds to just one x–y slice of the propellant pack, and other slices, unburned, are shown in Fig. 7; the top of each slice is nominally the burning surface. In Fig. 8 we see the instantaneous combustion field (temperature and streamlines) for four slices. The spacing between the arrows on the streamlines is proportional to the local gas speed, and it is apparent that the relatively cool gases over the large AP particles move more slowly than the hot gases elsewhere.

Figure 9, showing reaction rates, gives some measure of the three different flames and their combined effect. Here the vertical scale in the gas has been stretched by a factor of 5, because otherwise neither the primary diffusion flame contours nor the total heat output contours can be made out.

V. Burning of Sandwich Propellants

Sandwich propellant burning has been extensively studied in the laboratory, most notably by Price and his colleagues, with a large number of reports extending over many years. These reports are more than an observation record; they incorporate careful and deep interpretations of this record and provide substantial physical insight into the nature of heterogeneous propellant combustion.[12,23,24]

Typically, the burning surface of a sandwich recedes at constant speed with unchanging shape, shape that varies with the pressure and the thicknesses of the AP and binder slices. There are obvious ingredients of the model which affect this.

The overall configuration of the AP is affected by the vigor of the AP/binder reactions and how strongly they drive the local regression in comparison with that of pure AP. Nonhorizontal portions of the AP have a vertical regression speed that is greater than the regression speed normal to the surface; a horizontal portion of AP can regress at a speed different from that of pure AP if there is significant surface curvature, because this affects the heat conduction in the solid-phase thermal layer.

The shape of the binder-and here the issue is to what extent does it rise above or sink below the level of the surrounding AP-is controlled by the heat flux to the binder from the local flame structures, and the characteristic binder surface pyrolysis temperature. The latter is defined by

$$T_{\text{char}} = E_B/R_u \log A_B \tag{20}$$

so that

$$r_b = \exp[E_B/R_u T_{\text{char}} - E_B/R_u T] \tag{21}$$

Because the activation temperature E_B/R_u is large, modest deviations of the surface temperature from T_{char} lead to significant variations in the regression rate. Consequently, the binder positions itself so that the surface temperature is close to T_{char}. Reduce T_{char} and the binder will shrink from the hottest part of the combustion field; increase T_{char} and the binder will thrust towards the hottest part of the combustion field. This feature is demonstrated in Ref. 8.

Now it seems quite likely that the kinetics parameters and the pyrolysis parameters of our model could be adjusted to define an optimum match between the observed surface shapes and the predicted

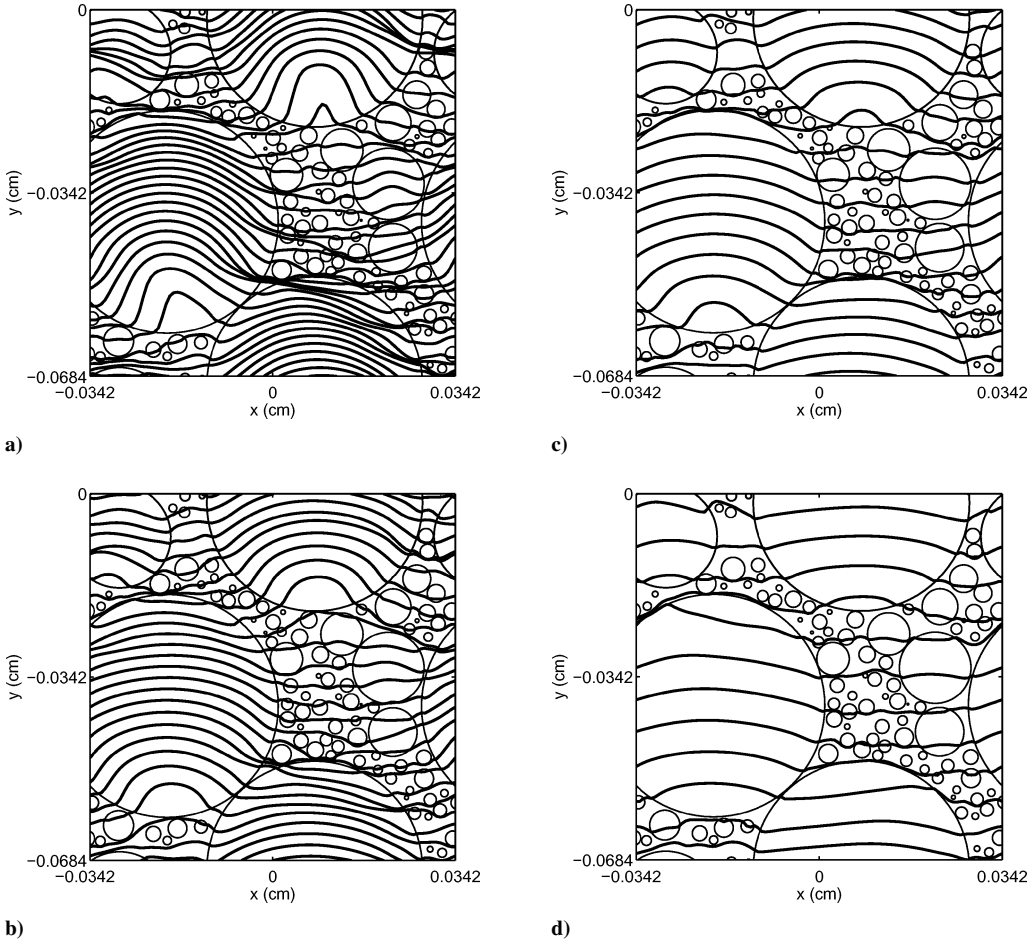

Fig. 6 The regressing surface of M21 at various times for four pressures: 20 atm (top left), 34 atm (top right), 68 atm (bottom left), 136 atm (bottom right). The $x - y$ slice is cut #7 of Figure 7, and the time interval between consecutive surface profiles is approximately 10^{-3} s.

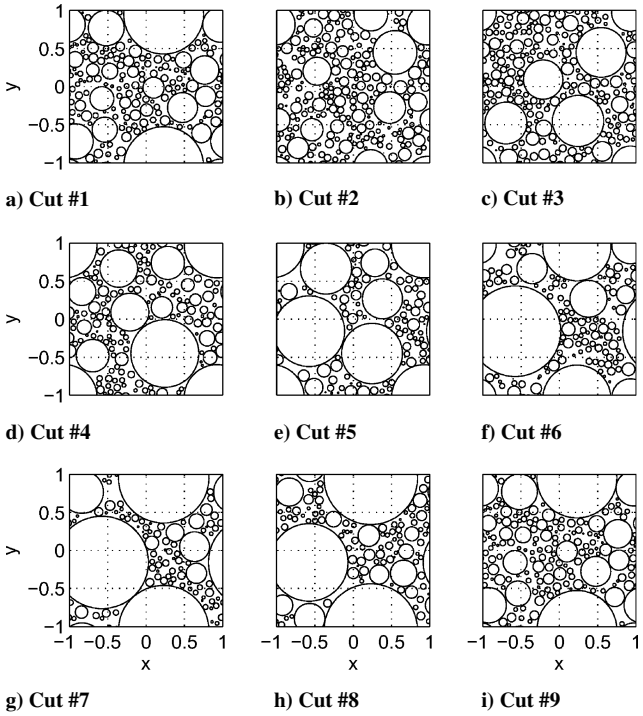

Fig. 7 Equally spaced slices through a pack that models M21. The last and first slices are at $z = \pm 1$, where, for this figure only, z, like x and y, is nondimensional.

shapes, with one caveat that we discuss later, but this would be far from an easy task. Even if we should choose the kinetics parameters to match pure AP burning and AP/binder blend burning, as we have described here, and just adjust the pyrolysis parameters to match surface shapes, note that a single change in the pyrolysis parameters requires a complete refitting of the kinetics parameters. And to what end? The same data set can not simultaneously be used for parameter fitting and for validation, and validation is the holy grail of modeling. In none of our work have we used multidimensional data to define parameter values, because our goal is to predict multidimensional behavior, and we wish to reserve for validation the small amount of multidimensional data, such as sandwich shapes, that is available.

It should be noted that there is another issue in the examination of sandwich data (the caveat of the previous paragraph). The numerical results are necessarily constructed for periodic sandwiches, an infinite array of alternating binder and AP slices, and the forcing of zero AP surface slope at the symmetry planes clearly has an impact on the overall surface shape. In contrast, almost all experimental data is for single isolated sandwiches (a binder slice between two AP slices), with ill-defined boundary conditions at each side. One would expect that if the binder is thin compared to the total sandwich thickness, the binder shape will be unaffected by the side boundary conditions, and comparisons are meaningful; recent work on triple sandwiches (nine AP and binder slices) appears to confirm this.[25] But whether more extensive comparisons are meaningful remains an open question.

With these points in mind we show in this section some results for sandwich combustion and comparisons with experimental observations from Ref. 12.

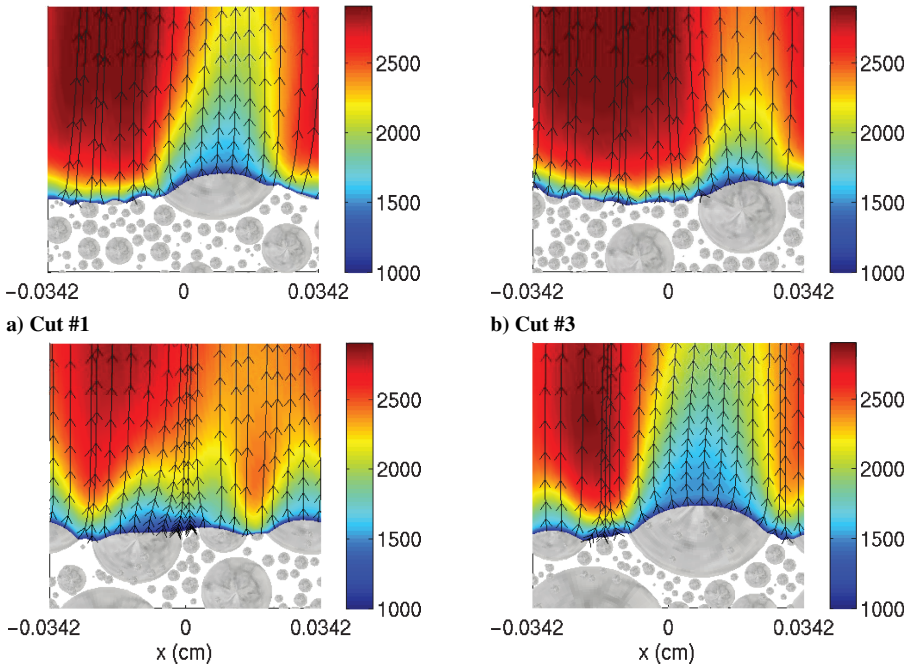

a) Cut #1 b) Cut #3

c) Cut #5 d) Cut #7

Fig. 8 The temperature field and streamlines at four slices of the burning M21 pack for a pressure of 34 atm.

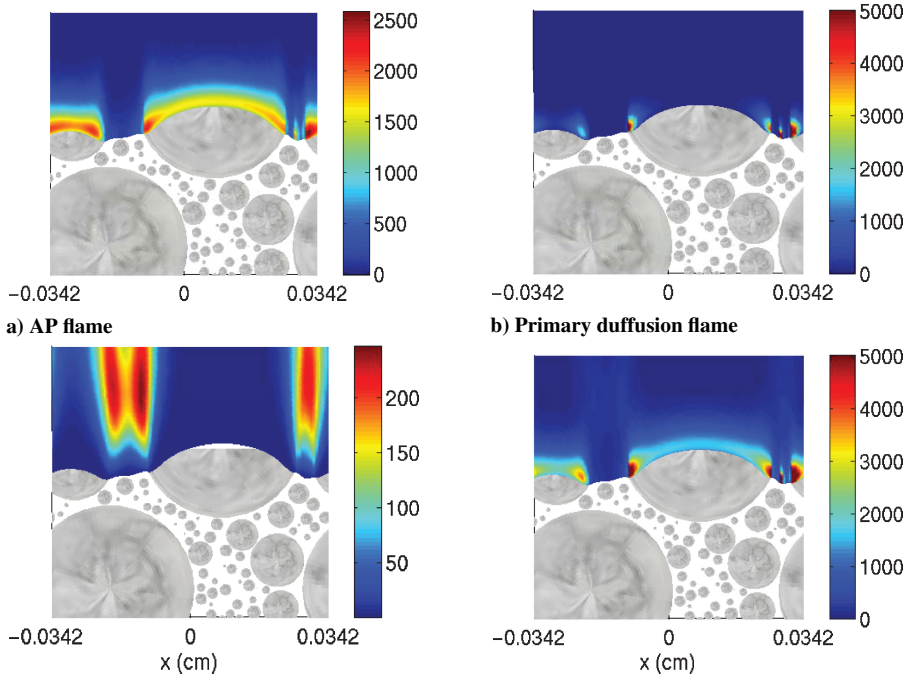

a) AP flame b) Primary duffusion flame

c) Secondary diffusion flame d) Total heat output

Fig. 9 The flame structure at cut #7 of the M21 pack for a pressure of 34 atm. Reaction rates are shown, as is the total heat output, equal to $Q_{g1} R_1 + Q_{g2} R_2 + Q_{g3} R_3$. The vertical coordinate in the gas phase is stretched fivefold.

Figure 10 shows the thermal field of a sandwich of width 600 μm with a binder thickness of 50 μm, burning at a pressure of 30 atm. This burns faster than pure AP so that the AP surface is nominally V-shaped, but the effect of the side symmetry boundaries on the AP surface shape is apparent and the convexity at these boundaries enhances the local burning rate, as required. The lines in this figure (red in the solid, black in the gas) are flux lines of the heat flux $-\lambda \nabla T$, and the spacing between the arrowheads on these lines varies inversely with the flux magnitude. The background is a color map of the temperature field, so that the flux lines are perpendicular to the level surfaces defined by the background. Note how the heat flows sideways high in the gas field, but is forced down toward the propellant surface by the symmetry boundaries. Note also that the flux lines in the solid converge near the symmetry boundaries, enhancing the heating of the solid that moves towards the surface, and it is for this reason that the locally convex AP surface regresses more rapidly than it would if level. This effect is one we noted in connection with Fig. 6.

Figure 11 shows the reaction fields corresponding to Fig. 10. Not surprisingly, the R_2 reaction (primary diffusion flame) is confined to a small portion of the combustion field, but it is intense and close to the surface and has a noticeable impact on the regression, as we

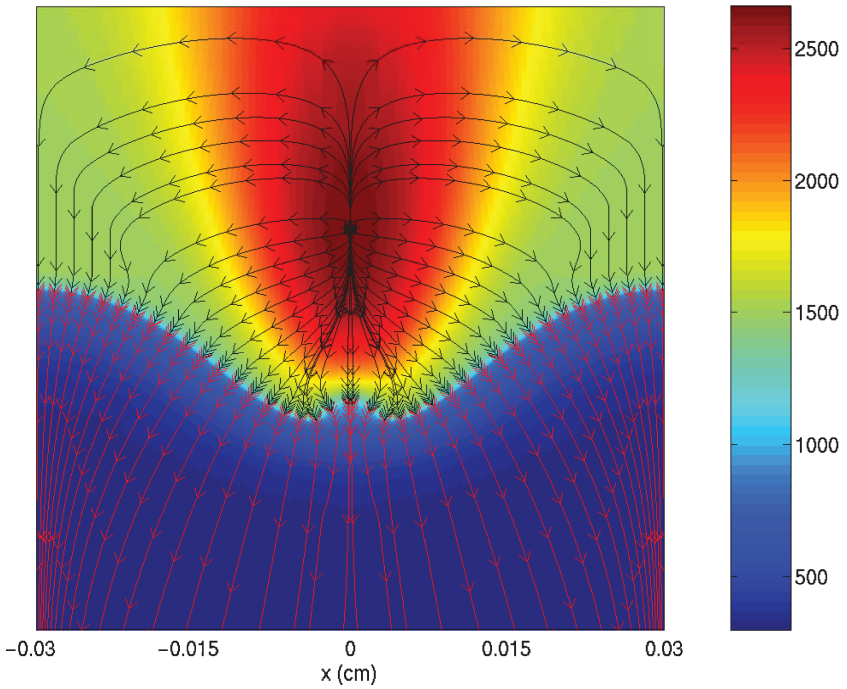

Fig. 10 Temperature field and flux lines of the vector $-\lambda\nabla T$ for a steadily burning sandwich: sandwich thickness 600 μm; binder thickness 50 μm; pressure 30 atm.

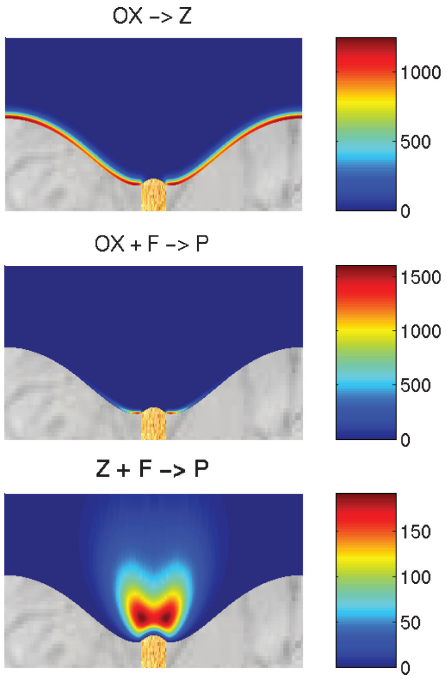

Fig. 11 Reaction-rate fields for the configuration of Figure 10.

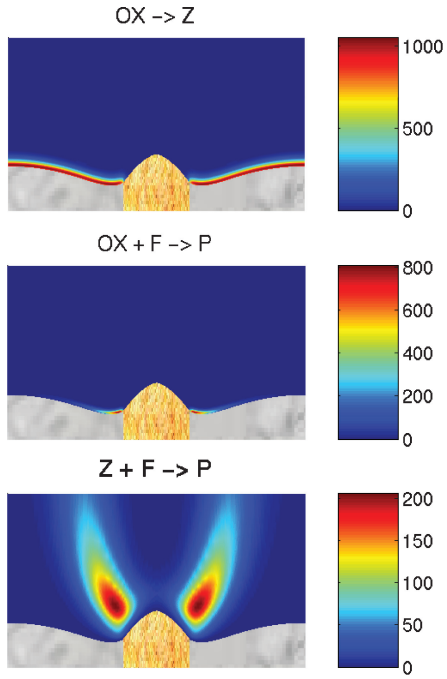

Fig. 12 Reaction-rate fields for a steadily burning sandwich: sandwich thickness 600 μm; binder thickness 130 μm; pressure 30 atm.

shall see. Figure 12 is the same as Fig. 11 but for a binder thickness of 130 μm.

If we compare the surface profiles of Figs. 11 and 12, it is clear that they are strongly influenced by the binder thickness, and Fig. 13 shows this effect for three different pressures. Note that as the pressure increases the binder tends to protrude more above the AP: apparently the center of the binder is insufficiently heated unless it moves farther out into the gas. At the same time, the difference between the regression speed and that of pure AP diminishes, hence the leveling of the AP surface at the higher pressures.

These trends shown are also part of the experimental record,[12] Fig. 14, although there are some obvious differences from the numerical results. A pressure of 7 atm is well below the AP self-deflagration limit (approximately 20 atm) and so, at that pressure, regions of AP remote from the diffusion flames do not regress. We believe that this could be captured by the numerical results if we turned off the AP pyrolysis when the surface temperature drops below the AP melting temperature, but this would need the level-set strategy[10] to accommodate the steep surface profiles and is something we plan to look at in the future. Figure 15 shows the surface temperature at 10 atm for both binder widths of Fig. 13. Although the temperature at the AP surface is everywhere lower than the melting temperature, it would be incorrect to conclude that

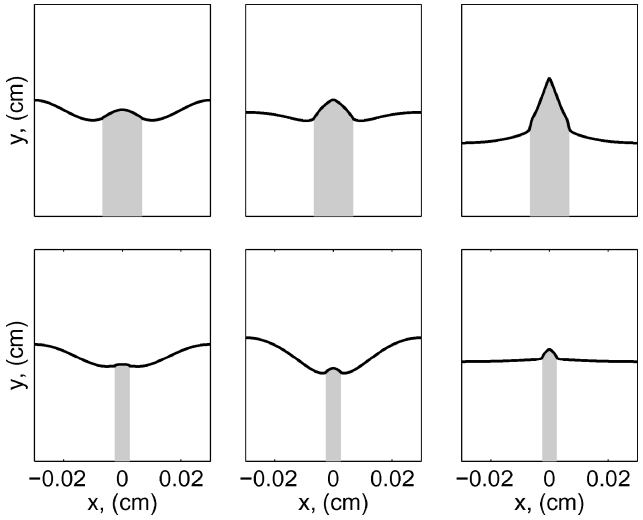

a) Press = 10 atm **b) Press = 35 atm** **c) Press = 120 atm**

Fig. 13 Numerical burning sandwich configurations for pressures of 10, 35, and 120 atm; binder widths 130 μm, 50 μm; total width 600 μm.

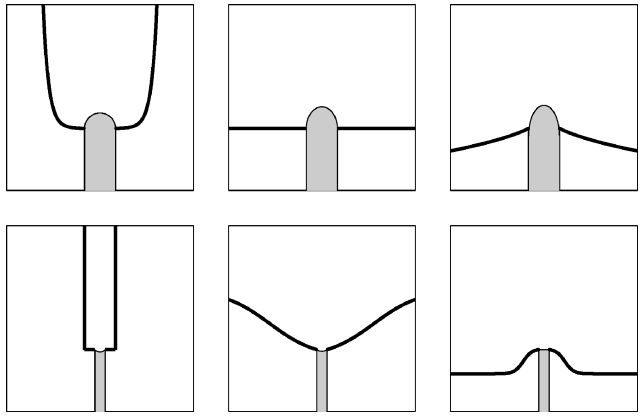

Fig. 14 Experimental burning sandwich configurations for pressures of 7, 35, and 100 atm; binder widths 150 μm, 50 μm; total width 600 μm. Redrawn from Fig. 2 of.[12]

these sandwiches cannot burn, for if a well were created by the ignition process this would undoubtedly have a significant effect on the surface temperature at the bottom of the well.

It might be sensible to use these low pressure configurations to refine some of the parameter values, leaving the higher pressure observations for validation, but refitting the kinetics parameters for each trial would be very time consuming.

Figure 16 shows the sandwich burning rates as a function of pressure. All three configurations (thin binder, thick binder, pure AP) burn at the same rate for pressures of 120 atm or higher.

VI. Importance of the Primary Diffusion Flame

The primary diffusion flame (R_2) occupies only a small fraction of the combustion field, but is more vigorous than the secondary diffusion flame (R_3), and so its importance is not clear from any of the results that we have presented so far. Figure 17 shows variations with pressure of the spatial integral of the two reactions for the two sandwiches; the solid lines correspond to R_3, the dashed lines to R_2. From this perspective it might be concluded, particularly for the thick binder, that R_2 could be switched off with little error for the sandwich calculations when blends are not used. But because the R_2 reaction zone is close to the surface, its role is not insignificant. Figure 18 shows the reaction-rate fields for the thin-binder sandwich burning at 30 atm when R_2 is switched off, to be compared to Fig. 11, and Fig. 19 shows the thick-binder results, to be compared to Fig. 12. Note that with R_2 switched off the AP surface

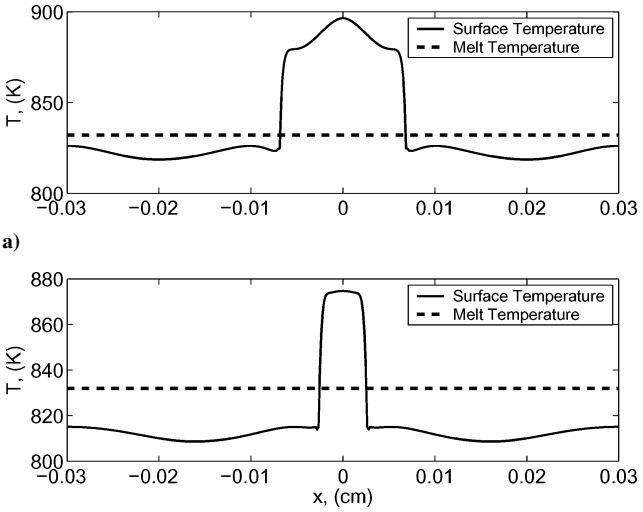

Fig. 15 Surface temperature at 10 atm for the thick binder (130 μm) sandwich (top) and the thin binder (50 μm) sandwich (bottom).

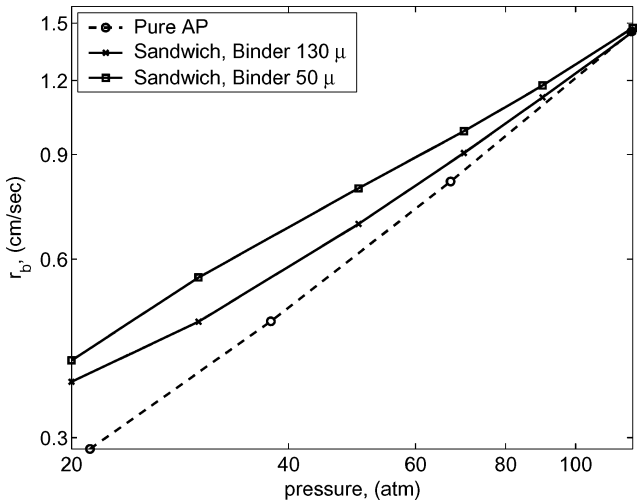

Fig. 16 Burning rate vs. pressure for the thin and thick binder sandwiches.

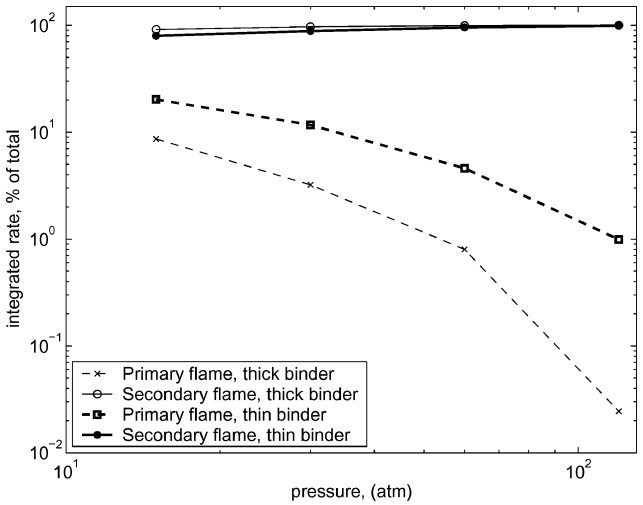

Fig. 17 Spatial integrals of R_2 (primary diffusion flame) and R_3 (secondary diffusion flame).

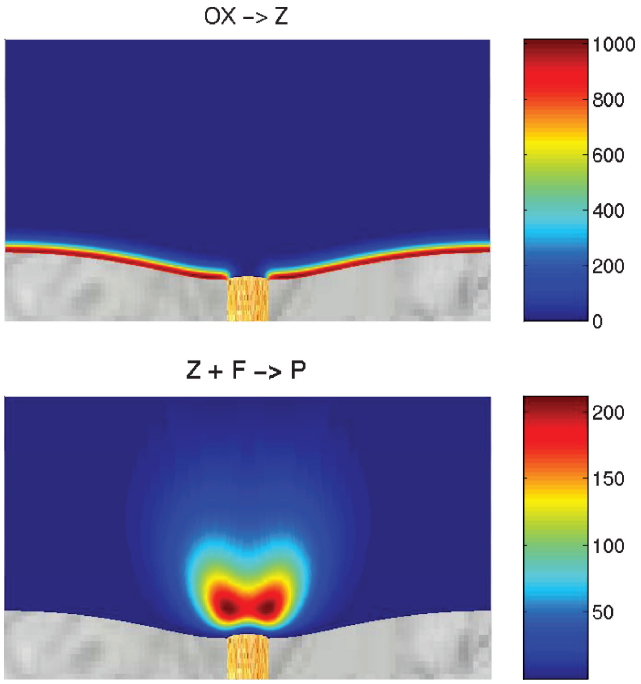

Fig. 18 Reaction-rate fields for the thin binder sandwich, pressure 30 atm, R_2 turned off; compare with Figure 11.

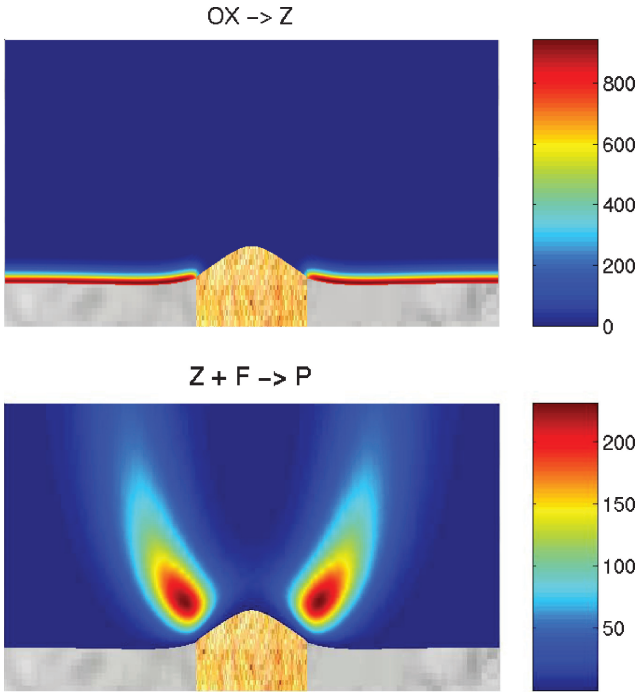

Fig. 19 Reaction-rate fields for the thick binder sandwich, pressure 30 atm, R_2 turned off; compare with Figure 12.

is significantly more level than it otherwise would be. In addition, there is a significant effect on the regression speeds, with the thin binder speed diminishing to 0.4378 cm/s from 0.558 cm/s, and the thick binder speed diminishing to 0.410 cm/s from 0.464 cm/s.

Conclusions

In this paper we have further developed our earlier work on propellant combustion, particularly Ref. 7, by adding a third reaction, the so-called primary diffusion flame. We have shown that this reaction can have a significant effect on burning rates. We note that three global reactions are a natural choice for this problem, in the same way that one global reaction is a natural choice for a simple diffusion flame or for a deflagration. In this connection it is unlikely that in our next paper on this subject we shall use a four-step model, or one with more steps, as the specification of such a model presents serious challenges. It would require an explicit recognition of some of the individual chemical constituents of the AP and binder, and strategies for specifying parameter values, strategies that are far from obvious. Moreover the stability issue discussed in Section III hangs over all such endeavors.

In examining the burning of Miller packs, Fig. 5, we have shown that for all except M21 (whose behavior appears anomalous) the agreement between theory and experiment is excellent. Some may argue that the prediction of steady-state burning rates is not a particularly demanding test, but it should be noted that all of our parameters are chosen from one-dimensional data and the differences in burning rates among the various packs, a consequence of three-dimensional morphology, and as much as three-fold, are accurately predicted.

General trends for the surface shape of steadily burning sandwich propellants are in approximate agreement with experiment, Figs. 13, 14. The shapes are affected by the choices of the pyrolysis parameters, and we have chosen not to fine-tune them to see if better agreement can be achieved. This partly reflects an aversion to curve-fitting exercises which all too often can be successful even if the underlying physics is wrong. One of the most difficult modeling challenges that faces us is a better treatment of the surface-an accounting of melt or foam layers, heterogeneous reactions, etc., rather than simple pyrolysis laws.

The ultimate value of the modeling reported here is not yet clear. Certainly it can not be used as a design tool of value to the industry in its raw form because of the magnitude of the computational task in determining just one point in Fig. 5. But recently we have shown, by averaging over a small region of the propellant surface, that it can be used to rationally derive a one-dimensional unsteady description, similar to but different from the classical QSHOD descriptions (see p. 856 of Ref. 21), that can be used in complete rocket simulations and accurately captures the influence of the subgrid combustion field on such computations.[1] And we have used it to discuss the classical problem of the burning response to acoustically generated pressure disturbances,[2] a problem that has hitherto defied serious theoretical treatment. Other applications exist, and will be addressed in due course.

Acknowledgment

This work was supported by the U.S. Department of Energy through the University of California under subcontract B523819. Any opinions, findings, and conclusions or recommendations expressed in this publication are those of the authors and do not necessarily reflect the views of the U.S. Department of Energy, the National Nuclear Security Agency, or the University of California. J. Buckmaster is also supported by the Air Force Office of Scientific Research and by the NASA Glenn Research Center. The packs used in the calculations were generated by S. Kochevets.

References

[1]Massa, L., Jackson, T. L., and Buckmaster, J., "Using Heterogeneous Propellant Burning Simulations as Subgrid Components of Rocket Simulations," *AIAA Journal*, Vol. 42, No. 9, 2004, pp. 1889–1900.

[2]Buckmaster, J., Jackson, T. L., Massa, L., and Ulrich, M., "Response of a Burning Heterogeneous Propellant to Small Pressure Disturbances," *Proceedings of the Combustion Institute*, Vol. 30, 2004, in press.

[3]Knott, G. M., Jackson, T. L., and Buckmaster, J., "The Random Packing of Heterogeneous Propellants," *AIAA Journal*, Vol. 39, No. 4, 2001, pp. 678–686.

[4]Kochevets, S., Buckmaster, J., Jackson, T. L., and Hegab, A., "Random Packs and Their Use in the Modeling of Heterogeneous Solid Propellant Combustion," *Journal of Propulsion and Power*, Vol. 17, No. 4, 2001, pp. 883–891.

[5]Chen, M., Buckmaster, J., Jackson, T. L., and Massa, L., "Homogenization Issues and the Combustion of Heterogeneous Solid Propellants," *Proceedings of the Combustion Institute*, Vol. 29, No. 2, 2002, pp. 2923–2929.

[6]Jackson, T. L., and Buckmaster, J., "Heterogeneous Propellant Combustion," *AIAA Journal*, Vol. 40, No. 6, 2002, pp. 1122–1130.

[7]Massa, L., Jackson, T. L., Buckmaster, J., and Campbell, M., "Three-Dimensional Heterogeneous Propellant Combustion," *Proceedings of the Combustion Institute*, Vol. 29, No. 2, 2002, pp. 2975–2983.

[8]Hegab, A., Jackson, T. L., Buckmaster, J., and Stewart, D. S., "Nonsteady Burning of Periodic Sandwich Propellants with Complete Coupling Between the Solid and Gas Phases," *Combustion and Flame*, Vol. 125, No. 3, 2001, pp. 1055–1070.

[9]Miller, R. R., "Effects of Particle Size on Reduced Smoke Propellant Ballistics," AIAA paper 82-1096, June 1982.

[10]Wang, X., Jackson, T. L., and Massa, L., "Numerical Simulation of Heterogeneous Propellant Combustion by a Level-Set Method," *Combustion Theory and Modelling*, Vol. 8, No. 2, 2004, pp. 227–254.

[11]Beckstead, M. W., Derr, R. L., and Price, C. F., "A Model of Composite Solid-Propellant Combustion Based on Multiple Flames," *AIAA Journal*, Vol. 8, No. 12, 1970, pp. 2200–2207.

[12]Price, E. W., Sambamurthi, J. K., Sigman, R. K., and Panyam, R. R., "Combustion of Ammonium Perchlorate-Polymer Sandwiches," *Combustion and Flame*, Vol. 63, No. 1, 1986, pp. 381–413.

[13]Massa, L., Jackson, T. L., and Short, M., "Numerical Solution of Three-Dimensional Heterogeneous Solid Propellants," *Combustion Theory and Modelling*, Vol. 7, No. 3, 2003, pp. 579–602.

[14]Beckstead, M. W., "Combustion Calculations for Composite Solid Propellants," *Proceedings of the 13th Jannaf Combustion Meeting*, Vol. 11, Chemical Propulsion Information Agency, Columbia, MD, CPIA Pub. No. 281, 1976, pp. 299–312.

[15]Beckstead, M. W., "An Overview of Combustion Mechanisms and Flame Structure of Advanced Solid Propellants," *Solid Propellant Chemistry, Combustion, and Motor Interior Ballistics*, edited by V. Yang, T. Brill, and W. Ren, Progress in Astronautics and Aeronautics, Vol. 185, AIAA, Washington, DC, 2000, pp. 267–286.

[16]Beckstead, M. W., "Solid Propellant Combustion Mechanisms and Flame Structure," *Pure and Applied Chemistry*, Vol. 65, No. 2, 1993, pp. 297–307.

[17]Rasmussen, B., and Frederick, R. A., Jr., "A Nonlinear Heterogeneous Model of Composite Solid Propellant Combustion," AIAA Paper 99-2228, June 1999.

[18]Cohen, N. S., and Strand, L. D., "An Improved Model for the Combustion of AP Composite Propellants," *AIAA Journal*, Vol. 20, No. 12, 1982, pp. 1739–1746.

[19]Jeppson, M. B., Beckstead, M. W., and Jing, Q., "A Kinetic Model for the Premixed Combustion of a Fine AP/HTPB Composite Propellant," *Proceedings of the 35th Jannaf Combustion Meeting*, Vol. 33, Chemical Propulsion Information Agency, Columbia, MD, CPIA Pub. No. 680, 1998, pp. 639–653.

[20]Zhou, X., Jackson, T. L., and Buckmaster, J., "A Numerical Study of Periodic Sandwich Propellants with Oxygenated Binders," *Combustion Theory and Modelling*, Vol. 7, No. 2, 2003, pp. 435–448.

[21]De Luca, L., "Theory of Nonsteady Burning and Combustion Stability of Solid Propellants by Flame Models," *Nonsteady Burning and Combustion Stability of Solid Propellants*, edited by L. De Luca, E. W. Price, and M. Summerfield, Progress in Astronautics and Aeronautics, Vol. 143, AIAA, Washington, DC, 1992, pp. 519–600.

[22]Williams, F. A., *Combustion Theory*, 2nd ed., Benjamin/Cummings, Menlo Park, CA, 1985, Chap. 9.

[23]Price, E. W., Handley, J. C., Panyam, R. R., Sigman, R. K., and Ghosh, A., "Combustion of Ammonium Perchlorate-Polymer Sandwiches," *AIAA Journal*, Vol. 19, No. 3, 1981, pp. 380–386.

[24]Price, E. W., "Effects of Multidimensional Flamelets in Composite Propellant Combustion," *Journal of Propulsion and Power*, Vol. 11, No. 4, 1995, pp. 717–728.

[25]Fitzgerald, R. P., Genevieve, P., and Brewster, M. Q., "Flame and Surface Structure of Laminate Propellants with Coarse and Fine Ammonium Perchlorate," AIAA paper 2003-1161, Jan. 2003.